AIP | Journal of Applied Physics

Pattern transformations in periodic cellular solids under external stimuli

K. Zhang, X. W. Zhao, H. L. Duan, B. L. Karihaloo, and J. Wang

Citation: J. Appl. Phys. **109**, 084907 (2011); doi: 10.1063/1.3567110
View online: http://dx.doi.org/10.1063/1.3567110
View Table of Contents: http://jap.aip.org/resource/1/JAPIAU/v109/i8
Published by the American Institute of Physics.

Pattern transformations in periodic cellular solids under external stimuli

K. Zhang,[1,2] X. W. Zhao,[1] H. L. Duan,[1] B. L. Karihaloo,[2] and J. Wang[1,a)]
[1]*State Key Laboratory for Turbulence and Complex Systems and Department of Mechanics and Aerospace Engineering, College of Engineering, Peking University, Beijing 100871, China*
[2]*School of Engineering, Cardiff University, Queen's Buildings, The Parade, Cardiff CF24 3AA, United Kingdom*

(Received 15 October 2010; accepted 13 February 2011; published online 21 April 2011)

The structural patterns of periodic cellular materials play an important role in their properties. Here, we investigate how these patterns transform dramatically under external stimuli in simple periodic cellular structures that include a nanotube bundle and a millimeter-size plastic straw bundle. Under gradual hydrostatic straining up to 20%, the cross-section of the single walled carbon nanotube bundle undergoes several pattern transformations, while an amazing new hexagram pattern is triggered from the circular shape when the strain of 20% is applied suddenly in one step. Similar to the nanotube bundle, the circular plastic straw bundle is transformed into a hexagonal pattern on heating by conduction through a baseplate but into a hexagram pattern when heated by convection. Besides the well-known elastic buckling, we find other mechanisms of pattern transformation at different scales; these include the minimization of the surface energy at the macroscale or of the van der Waals energy at the nanoscale and the competition between the elastic energy of deformation and either the surface energy at the macroscale or the van der Waals energy at the nanoscale. The studies of the pattern transformations of periodic porous materials offer new insights into the fabrication of novel materials and devices with tailored properties. © *2011 American Institute of Physics*. [doi:10.1063/1.3567110]

I. INTRODUCTION

Cellular solids, which are common in nature, have been widely used in engineering practices due to their special mechanical and physical properties. The porous pattern of the cellular materials plays an important role in determining their properties.[1–5] Recently, much attention has been paid to the periodic porous materials at nano- and micron-scales because of their potential use as photonic crystals,[6] tunable hydrophobic surfaces,[7] and so on. Among nanoporous materials, the single-walled carbon nanotube (SWCNT) bundles, which can be regarded as crystals with a two-dimensional triangular lattice structure,[8–10] have potential applications in various nanoscale devices.[8,11]

It is well-known that changes in structural patterns can be triggered by elastic instability at the macroscale.[3] However, the mechanical behavior of the materials at the nanoscale is different from those at the macroscale due to the surface effect.[12–14] Furthermore, as the patterns found in nature are so varied and complex, it is likely that there are other mechanisms for pattern transformation at work besides the elastic instability. A deep understanding of these mechanisms at different scales would help to control self-assembly and fabrication of devices with transformative properties. Here, we investigate the dramatic pattern transformations that occur under external stimuli in a class of simple periodic cellular structures that include a nanotube bundle and a millimeter-size plastic tube bundle. We conclude that there are five possible mechanisms for the pattern transformation at different scales.

a)Author to whom correspondence should be addressed. Electronic mail: jxwang@pku.edu.cn.

II. METHOD

A. Nanotube bundle

1. Density functional theory calculation

The density functional theory (DFT) was employed to investigate the pattern transformation of SWCNT bundles under compressive deformation. A crystal of (12, 12) SWCNT bundle (with a radius of 16.27 Å) with a hexagonal packing mode was investigated with the software CASTEP.[15,16] A plane-wave basis set, Vanderbilt ultrasoft pseudopotentials, and generalized gradient approximation (GGA) were applied. To optimize the structure, a cutoff energy of 340 eV, 3 k-points, and a force on each carbon atom less than 0.02 eV/Å were adapted. The SWCNT bundle was modeled by a rectangular representative unit containing two tubes with periodic boundary conditions. The bundle was compressed perpendicular to the axis of the tubes with up to 20% strain applied either gradually in 14 steps or in a single step. In every step of the DFT calculation, the hydrostatic compression was introduced by decreasing the length of the crystal lattice parameter a, together with a proportional decrease in the lattice dimension b. The lattice dimension c was unchanged since SWCNTs are highly stiff along the axial direction (a,[1,0,0], b[1,2,0], and c[0,0,1]). Thus, the in-plane stresses in the cross-section of the tube can be considered to be approximately equal. A similar setup has been used in a study by Chan *et al.*[17] Then, all the atoms in the unit were fully relaxed, which means that the system has sufficient (infinite) time to respond to the strain. Thus the deformation implemented gradually in 14 steps can be considered as being quasistatic. Since the one-step deformation to 20% strain had a deformation rate about one order of magnitude

higher than the gradual deformation, it was reasonable to consider the one-step deformation to be a sudden loading.

2. Continuum analysis

We also carried out an analytical continuum analysis of the deformation modes of the SWCNT bundle, and compared the results with the above DFT calculations. In this continuum model, the eigenvalues of the buckling modes of a circular tube under a gradual radial loading were obtained analytically. The nanotubes in the bundle were in a state of plane strain because they were highly stiff in the axial direction. One nanotube in the SWCNT bundle is surrounded by six nanotubes; thus a single nanotube can be regarded as a circular tube under six equal radial loads, representing the repulsive forces from the six neighboring tubes. The buckling loads of the (12, 12) nanotube under the 6 radial loads are given by $P_{cr} = -(k^2 - 1)Eh^3/[12(1 - \nu^2)R^2]$ (Ref. 18) for the quasistatic loading case. The radius R of a (12, 12) nanotube is 8.135 Å, which is the same as the radius modeled by the DFT. The thickness h, elastic modulus E, and Poisson's ratio ν are 0.66 Å, 5.5 TPa, and 0.19, respectively.[19–21] If the equal radial point loads are applied suddenly, the buckling mode number is given by the nearest integer to $k^* = \sqrt{1.5P/P_{cr1}}$,[22] where P is the magnitude of each of the equal radial forces applied suddenly, and P_{cr1} is the buckling load for the first mode under the quasistatic loading case.

In order to ascertain whether elastic buckling of the SWCNT can occur under the van der Waals interactive forces on the tubes when either the gradual compressive strain up to 6% or the 20% sudden compressive strain was applied on to the bundle, we used the Lennard–Jones 6–12 pair potential to calculate the van der Waals interaction energy between two atoms $u(x) = -A/x^6 + B/x^{12}$, where A and B are 15.2 eV × Å^6 and 24.1 × 10^3 eV × Å^{12}, respectively.[19,23,24] The interactive force on each atom is then given by $F(x) = du(x)/dx = 6A/x^7 - 12B/x^{13}$. By comparing the elastic buckling loads obtained previously with the interactive forces on the tubes, we can ascertain whether the SWCNT bundle will buckle or not.

B. Plastic straw bundles

1. Experiment

We arranged polypropylene plastic straws (diameter = 6 mm; wall thickness = 0.2 mm; melting point = 90 °C) in a hexagonal close-packed pattern, exactly as the carbon nanotubes in Sec. II A, and tied the bundle with a thin metal strap. We then heated the bundle past the melting point in two ways: by conduction through a base heating plate (that is, by heating one end of the bundle) and by convention in a chamber furnace at the rate of 10 °C/min and observed the pattern transformations in the plastic straw bundle. Note that the conduction mode of heating raised the temperature above the melting pointing of the plastic straw faster than the convection mode.

2. Theoretical analysis

To explain the observed pattern transformations, two models were used: an elastic buckling model of a circular tube, and a fusion model of the plastic tube walls.

The elastic buckling of a circular plastic tube under gradually applied radial loads was studied analytically. As the plastic tubes in the bundle were free to move in the axial direction, they can be regarded to be in a state of plane stress. As the straws form a hexagonal close-packed arrangement, a plastic straw in the bundle can be considered to be under six radial concentrated loads or uniform pressure along its circumference. The buckling loads under these two radial loading configurations are given by $P_{cr} = -(k^2 - 1)Eh^3/(12R^2)$ and $q_{cr} = -(k^2 - 1)Eh^3/(12R^3)$, where R, h, and E are the radius, the thickness, and the elastic modulus of the circular plastic tube, and k is the mode number; $k = 1$ corresponds to the rigid body mode.[18] The elastic modulus is 1.389 GPa.[25] Next, we calculated the radial compressive force resulting from the constrained expansion of a plastic straw surrounded by six straws. Consider a single circular plastic straw surrounded by six identical plastic straws that experiences a temperature rise from 23 °C to 90 °C; thus each of them would expand radially by the amount $u_r = 28.14$ μm (coefficient of thermal expansion of plastic = 1.4 × 10^{-4}/°C),[25] but this expansion is constrained by the metal strap. As a result the innermost plastic straw in the bundle is subjected to a radial compression equal to $p_o = -Eu_r/[R(\nu - r')]$, where the Poisson ratio ν of the plastic is 0.38[25] and r' stands for $[R^2 + (R - h)^2]/[R^2 - (R - h)^2]$.[26] This radial compression is compared with the above buckling load to ascertain the buckling mode of the straw in the bundle.

The model for the fusion of the plastic straw walls follows the analysis in the work of Oruganti and Ghosh.[27] In this model [see Fig. 6(e)], the negative pressure q in the liquid bridge with the concave meniscus, the tensile stress σ_t, the strain ε_t, and the strain rate $\dot{\varepsilon}$ in the wall of the straw are given by

$$\begin{aligned} q &= \frac{\gamma}{\rho} \\ \sigma_t &= \frac{\gamma r}{\rho h} \\ \varepsilon_t &= (2\sqrt{3} - \pi)\frac{R_o - r}{\pi R_o} \\ \dot{\varepsilon} &= -\frac{2\sqrt{3} - \pi}{\pi r}\frac{dr}{dt} \end{aligned} \tag{1}$$

where ρ is the radius of the semicylindrical meniscus, γ is the surface tension of the liquid (or semisolid), and h is the thickness of the wall of the plastic tube. R_o and r are the mean radii of the original and deformed straw at time t, respectively. The expression of the tensile stress in equation (1) is different from the work of Oruganti and Ghosh.[27] We obtained this expression from the equilibrium condition, whereas an inappropriate equilibrium condition seemed to have been used in the work of Oruganti and Ghosh.[27] We assumed that the plastic of the straw behaves as a linear visco-elastic material when the temperature was beyond its melting point. The response of such a material is usually expressed in terms of the effective stress $\bar{\sigma}$ and effective strain $\bar{\varepsilon}$.[27] For the plane stress state, these are given by

$$\bar{\sigma} = \sigma_t, \bar{\varepsilon} = \frac{2(1 - \nu)}{3}\varepsilon_t, \bar{\sigma} = 3\eta\dot{\bar{\varepsilon}} \tag{2}$$

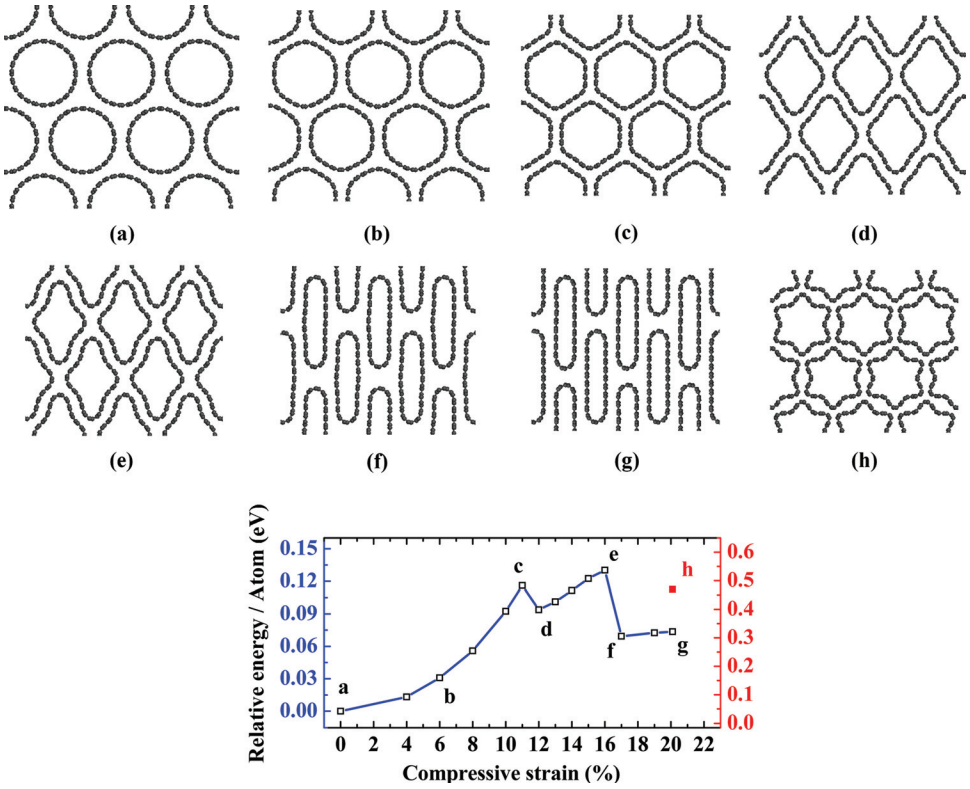

FIG. 1. (Color online) Dramatic pattern transformations of a SWCNT bundle during compression.

where η is the shear viscosity. Substituting Eq. (1) into Eq. (2) gives $\dot{r} = -br^2/\rho$, where b is equal to $\pi\gamma/[(4\sqrt{3}-2\pi)h(1-\nu)\eta]$. The solution of this differential equation

$$r = \frac{\rho R_o}{\rho + btR_o} \tag{3}$$

describes how the radius of the straw evolves with time.

III. RESULTS

A. Pattern transformation in SWCNT bundles

As mentioned in Sec. II A 1, the (12, 12) SWCNT bundles were analyzed using the DFT under external compression up to a 20% compressive strain applied in two ways. When the compression is applied gradually, the cross-section of the SWCNT bundle undergoes several pattern transformations (Fig. 1) as the relative energy, i.e., the total energy relative to the energy without the external pressure, is increased. The circular cross-section of the tubes under no external pressure gradually changes into a rounded hexagon when the strain has reached 6% (point b in Fig. 1). The existence of a hexagonal structure has been proved by theory and experiment.[9,19,23,28–30] The deformed shape is further accentuated when the strain is increased beyond 6%. Interestingly, a new rounded tetragonal structure (point d in Fig. 1) has been triggered from the hexagonal shape, with a corresponding drop in the total energy. As the strain is further gradually increased, the cross-section of the tube goes through a shape transformation for the third time with a decrease of energy; it changes from the rounded tetragonal shape into a flattened structure similar to a 400 m running track (points f and g in Fig. 1). The flattened structures have also been observed in other nanotube bundles such as (6, 6), (8, 8) and (10, 10).[17] It has been reported that the flattened structure of the nanotube is the most favored structure.[17] The intermediate rounded-tetragonal states are not preferred.

On the other hand, when the strain of 20% is applied in one step to the SWCNT bundle, an amazing new hexagram pattern (point h in Fig. 1) is triggered from the circular shape. A comparison of the relative energy of the hexagram pattern (right-hand scale) with that of the flattened structure at the same strain of 20% (point g, left-hand scale) shows that it is more than six-fold larger (0.47 eV/atom against 0.075 eV/atom).

B. Pattern transformation in plastic straw bundles

A close-packed hexagonal plastic straw bundle is shown in Fig. 2(a). Figures 2(b) and 2(c) show that the circular plastic straw bundle is transformed into a hexagonal pattern on heating through the baseplate, and then into a hexagram pattern when heated by convection for 3 min. These patterns are similar to those of the nanotube bundle at points b and h (Fig. 1).

IV. DISCUSSION AND CONCLUSIONS

We now examine several mechanisms of pattern transformation.

A. Elastic instability at different scales

Elastic bodies can transform their cross-sectional shape by elastic instability under quasistatically applied external loading. Figure 3 shows the first five eigen-modes of a circular elastic tube subjected to six equal radial point loads (for details, see Secs. II A 2 and II B 2).[18] The circular tube has

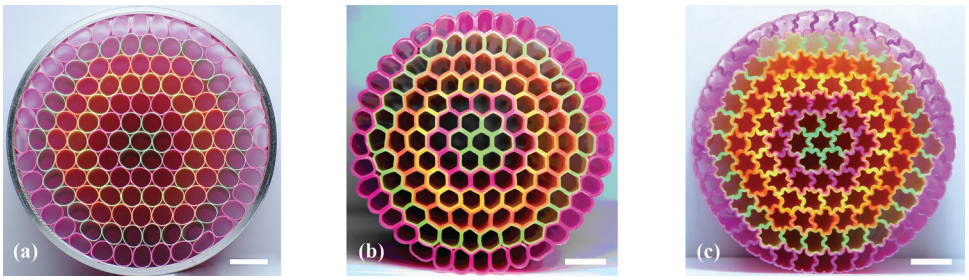

FIG. 2. (Color online) Pattern transformation of millimeter-size plastic straw bundle: (a) A bundle of closed-packed circular plastic straws tied by a thin metal strap. (b) A perfect hexagonal honeycomb pattern triggered by heating through the baseplate. (c) A hexagram pattern triggered by heating in a furnace. Scale bar is 12 mm.

the same first five eigen-modes, if instead of six equal radial point loads it is subjected to a uniform radial pressure, e.g., a hydrostatic pressure.

A single carbon nanotube in the SWCNT bundle of Fig. 1 can be regarded as a circular tube under the intertube van der Waals interactions with the surrounding six nanotubes (Fig. 4). In other words, the starting configuration of the SWCNT bundle is identical to the model of Fig. 3(a). The elastic buckling modes for the (12, 12) nanotube under six equal radial point loads were calculated by the theory of elastic stability[18] (Sec. II A 2). The buckling modes are identical to those shown in Fig. 3 and the corresponding buckling loads for the first five modes are −0.63, −1.68, −3.15, −5.04, −7.35 N/m, respectively (here, and elsewhere in the following, the negative sign implies compression). It is not surprising therefore that the patterns triggered in the SWCNT bundle (the rounded tetragon, the flat 400 m track, and the hexagram) have features that are similar to the buckling eigen-modes of a circular nanotube in the bundle. Recently, it has been found that a single circular nanotube can transform into an ellipse under very high pressure.[31] Thus, we can conclude that elastic buckling plays a role in the shape transformation of both a single nanotube under hydrostatic pressure and a nanotube bundle.

The complex hexagram pattern of the nanotube bundle (point h in Fig. 1) is also the result of elastic buckling. When the 20% strain is suddenly applied to the tube bundle, the center to center distance between the tubes is reduced instantaneously by 20% and the van der Waals interactive forces on each of the atoms in the tube can be calculated on basis of the Lennard–Jones 6–12 pair potential model (Sec. II A 2). The six atoms in Fig. 4 were chosen to calculate the interactive forces. We also calculated the forces on the atoms along the radial direction, as shown in Fig. 5(a). In order to be able to compare the atomistic results with the previously obtained two-dimensional plane strain eigen-value analysis, the radial forces in the atomistic model need to be averaged first in the direction of the tube axis. Because the pairs of atoms 1 and 2, 3 and 4, and 5 and 6 are arranged periodically along the tube axis approximately in a straight line, it is reasonable to add the forces on the pairs of atoms 1 and 2, 3 and 4, and 5 and 6 and then to divide the sum by the period n [$n=0.2425$ nm, Fig. 4(b)]. The averaged force on each atom along the radial direction of the atomistic model obtained in this manner is shown in Fig. 5(b). It is the same at all sections along the axial direction of the tube, as in the eigen-value analysis. A nanotube in the bundle under the sudden application of 20% strain is therefore similar to the circular tube under six concentrated radial forces, each of magnitude $P=F_{\text{atom56}}+2F_{\text{atom34}}\cos 15^{\circ}+F_{\text{atom12}}\cos 30^{\circ}=-11.85$ N/m applied suddenly. We now calculate which buckling mode the tube will take under this sudden loading (Sec. II A 2). We find k^{*} to be equal to 5.3, so that the tube should transform into mode 4 (buckling mode number 5, Fig. 3). However, because of the hexagonal symmetry of the nanotube bundle, it will actually transform into the hexagram pattern (mode 5, Fig. 3). This is consistent with the hexagram pattern of the nanotube bundle (point h in Fig. 1) obtained by the DFT calculation.

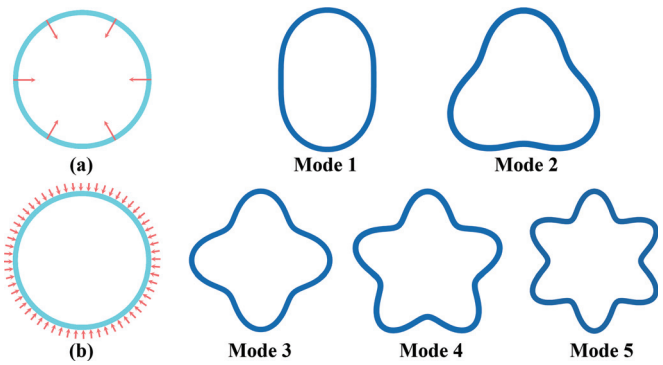

FIG. 3. (Color online) The first five eigen-modes of a thin circular tube subjected to (a) equal radial point loads or (b) uniform hydrostatic pressure. For the millimeter-size plastic tube, each of the six radial point loads are −0.33, −0.88, −1.65, −2.64, and −3.85 N/mm, respectively, and the corresponding hydrostatic pressure levels are −0.110, −0.293, −0.550, −0.880, and −1.283 MPa, respectively. For the nanotube, the buckling load corresponding to the first five buckling modes under the six equal radial point loads are −0.63, −1.68, −3.15, −5.04, and −7.35 N/m, respectively.

B. Minimization of the surface energy at the macroscale or of the van der Waals energy at the nanoscale

The intertube van der Waals interaction of a circular nanotube in a SWCNT bundle with the surrounding nanotubes has been found to transform it into a rounded hexagon

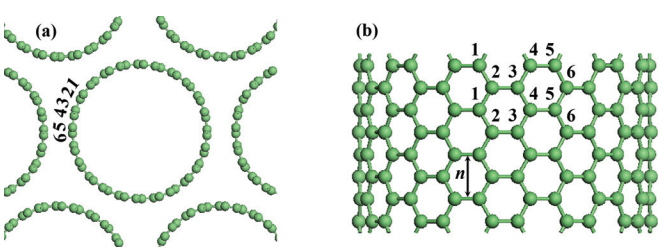

FIG. 4. (Color online) (a) Arrangement of the atoms in a (12, 12) nanotube, showing the six representative atoms. (b) Periodicity of atomic pairs along the tube axis. $n=0.2425$ nm.

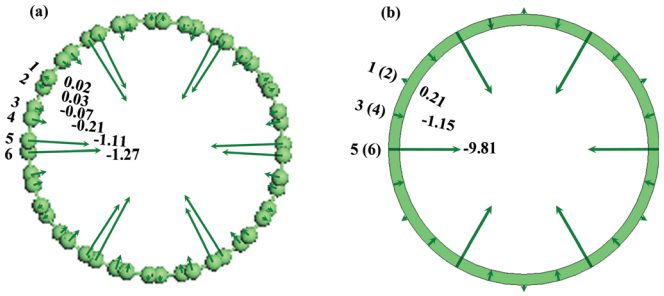

FIG. 5. (Color online) (a) Force distributions on the atoms of the (12, 12) nanotube along the radial direction under 20% strain. Unit is nN. (b) Forces on pairs of atoms averaged over the period n along the axial direction. Unit is N/m.

in order to minimize the van der Waals energy at the nanoscale.[10,19,23]

The hexagonal close-packed configuration of the circular plastic tube bundle resulting from heating through a baseplate [Fig. 2(b)] is a consequence of minimizing the surface tension at the macroscale. When the circular plastic straws are heated to 90 °C, their surfaces begin to melt and become wavy as a result of surface tension [Figs. 6(a) and 6(b)]. A liquid (or a semisolid) bridge with a concave meniscus is formed at the triple junctions between neighboring plastic straws.[27] The mean radius ρ of the concave meniscus for the plastic straw is 25 μm [Fig. 6(c)]. As a result of the surface tension of this bridge, a negative pressure is created in the junction that in turn leads to a tensile state of stress in the straw walls [Fig. 6(e)]. The walls are thus continuously stretched during this process. In time, the adjoining walls fuse together increasing the contact area and forming a homogeneous interface [Figs. 6(c)–6(e)]. This process continues until the entire curved walls become planar minimizing the surface energy. We now follow the model of the fusion of straw walls induced by melting, described in Sec. II B 2. It is clear from Eq. (3) that a sharp corner ($r=0$) would take infinitely long to evolve. In a limited span of time, a single circular straw in a hexagonal bundle can therefore be expected to become a hexagon with rounded but not sharp corners. As seen from Fig. 6(d), the radius of the rounded corners of the hexagonal cell is 0.42 ± 0.19 mm. The time it takes for the pattern formation from an initial radius R_o to a nonzero radius r_f is given by Eq. (4)

$$t = \frac{\rho}{b}\left(\frac{1}{r_f} - \frac{1}{R_o}\right). \tag{4}$$

For the polypropylene of the straw bundle considered here, the surface tension and the Poisson ratio are 22.5×10^{-3} N/m and 0.38, respectively,[25] and its shear viscosity is in the range from 2×10^4 Pa s to 3.3×10^5 Pa s depending upon its molecular weight.[32] Thus, the time taken for the formation of the rounded hexagonal pattern will be from 1.2 s to 19 s. Eq. (4) shows that the time will increase with the increasing diameter of the tube, so that the pattern transformation in microstraws will be much more rapid than in macrostraws. We believe this mechanism may also be responsible for the hexagonal cell pattern in natural honeycombs.[33]

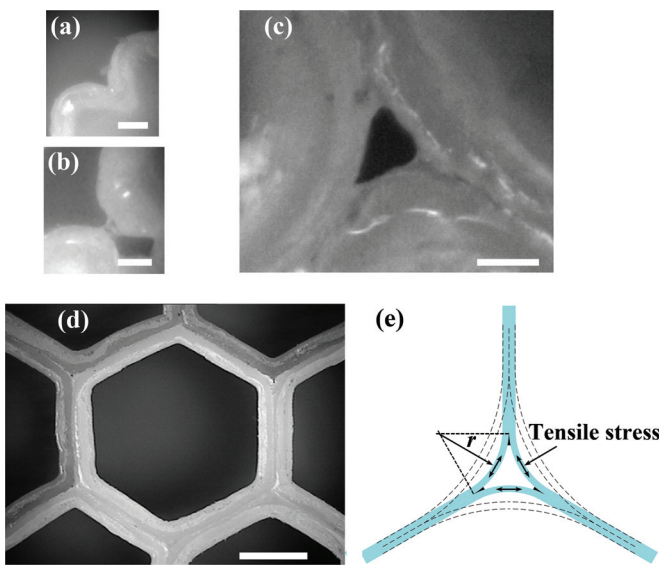

FIG. 6. (Color online) Process of transformation of a close-packed circular tube bundle into a perfect hexagonal close-packed structure: (a) A circular plastic straw with wavy sides due to surface tension, scale bar is 90 μm. (b) Two walls from neighboring tubes fuse together, scale bar is 55 μm. (c) A triple junction during the process of transformation, scale bar is 100 μm. (d) Final rounded hexagonal pattern a single circular tube in the plastic tube bundle, scale bar is 2 mm. (e) Schematic diagram of a triple point during the process of transformation.

C. Competition between two mechanisms

The complex pattern of the nanotube bundle is a result of the competition between the van der Waals energy of intertube interaction and the elastic energy of deformation of the tubes in the bundle induced by the distortion of the intratube atomic arrangement under applied compression.[19] The van der Waals interaction energy favors polygonization into a hexagon,[19,23] while the buckling instability leads the cross-section of the tubes into one of the eigen-modes under six radial point loads (Fig. 3).

The interactive force on each atom of the (12, 12) nanotube under gradually increasing strain up to 6% (point b in Fig. 1) has also been calculated by the atomistic model described above. As shown in Fig. 7, the distribution of the force along the radial direction is similar to that under the suddenly applied strain of 20%, but the maximum concentrated radial force is only $P = F_{\text{atom56}} + 2F_{\text{atom34}} \cos 15^{\circ}$

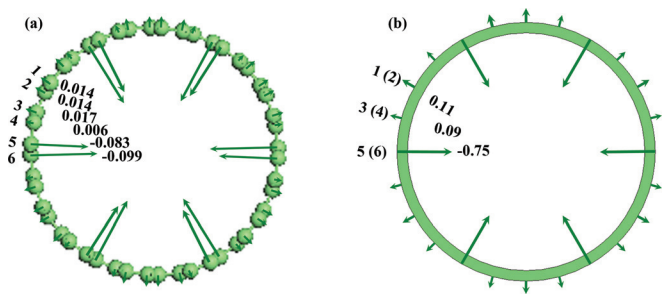

FIG. 7. (Color online) (a) Force distributions on the atoms of the (12, 12) nanotube along the radial direction under the gradually increasing strain of 6%. Unit is nN. (b) Forces on pairs of atoms averaged over the period n along the axial direction. Unit is N/m.

$+F_{\text{atom}12}\cos 30^{\circ} = -0.48$ N/m, which is less than the buckling load −0.63 N/m for the first mode (Fig. 3). The tube will therefore not transform into the flattened pattern (mode 1 in Fig. 3). At this strain level, the elastic energy of deformation is too small, and the van der Waals interaction plays the principal role in the pattern transformation. As a result, the nanotubes in a bundle transform into the hexagonal pattern which is consistent with the results of the DFT calculation.

It has been reported that a nanotube bundle without any pressure will remain circular in shape or polygonize into a hexagon or collapse into an elliptical shape depending on the radius of the tube.[9,10,19,23,34] Furthermore, the symmetry of the nanotube will determine the radial loading and its eigenmodes. Thus, the symmetry, the radius, and the chirality of the tube all have an important role in the competition between the van der Waals energy of intertube interaction and the elastic energy of deformation of the tubes in the bundle.

This competition is also at work in the plastic straw bundle heated in a chamber furnace. Now of course, it is the competition with the surface energy rather than the van der Waals interaction energy. When the plastic straws in the bundle are first heated they expand and compress one another. The temperature of the circular straw does not reach its melting point as rapidly under the convection heating in the furnace as it did under the conduction heating through the baseplate. Thus, the wall of the straw does not melt or adhere to the walls of the adjoining straws at the beginning of the heating process. Therefore, the liquid bridge has not yet formed at the triple junction. However, the circular straws in the interior of the close-packed bundle can experience radial compressive forces from the surrounding expanding straws because their free radial expansion is constrained by the metal strap. Although the bundle is heated uniformly in the chamber furnace, the plastic straws near the metal strap will heat faster than those in the interior of bundle. However, as seen from Fig. 2(c), the straws in the interior of the bundle have all very nearly the same hexagram pattern, indicating that the boundary effect induced by the metal strap can be ignored in that region. The model of a single circular plastic straw under hydrostatic pressure can be used to explain its transformation into the hexagram pattern (Sec. II B 2). If we assume that the outer radius of this straw remains unchanged, then it must experience a hydrostatic compression equal to −0.922 MPa. Although this pressure is less than the buckling load of −1.283 MPa corresponding to the hexagram pattern (mode 5, Fig. 3), it is known that the buckling load is considerably reduced by any imperfections in the plastic straw wall.[22] Thus, we can conclude that the straw will not retain its shape but it will transform into the hexagram pattern (mode 5). Subsequently, the surfaces of the straws melt, forming a liquid bridge at the junctions leading to the fusion of the walls of adjoining straws.

The systematic studies of the pattern transformations in periodic porous materials offer new insights into the manufacture and application of novel materials and devices. However, the surface energy of the solid materials at the macroscale is negligible in comparison with that of liquids. Thus, it is difficult for solid porous materials to reduce the surface energy by fusion. Pattern transformation of the nanotube bundle by external stimuli can result in increasing compressibility and other novel physical and chemical properties,[9,19,35,36] with many potential applications.

Novel shape transformations in a class of periodic porous materials have been investigated at the nano- and macroscales. The mechanisms which prompt these transformations have been identified; these are the elastic instability, which is possible at all scales; the minimization of the surface energy at the macroscale, the minimization of the van der Waals energy at the nanoscale; the competition between the elastic energy of deformation and the surface energy at the macroscale; and the competition between the elastic energy of deformation and the van der Waals energy at the nanoscale.

ACKNOWLEDGMENTS

We thank the National Natural Science Foundation of China (Grant Nos. 10525209, 10872003, and 10932001), the China-UK Science Network Scheme of the Chinese Scholarship Council and The Royal Society, London, and the Foundation for the Author of National Excellent Doctoral Dissertation of China (FANEDD, Grant No. 2007B2) for financial support.

[1] L. J. Gibson and M. F. Ashby, *Cellular Solids: Structure and Properties*, 2nd ed. (Cambridge University Press, Cambridge, U.K., 1997).
[2] P. Ball, *The self-made tapestry: Pattern Formation in Nature* (Oxford University Press, New York, 1999).
[3] T. Mullin, S. Deschanel, K. Bertoldi, and M. C. Boyce, Phys. Rev. Lett. **99**, 084301 (2007).
[4] K. Bertoldi and M. C. Boyce, Phys. Rev. B **77**, 052105 (2008).
[5] K. Bertoldi, M. C. Boyce, S. Deschanel, S. M. Prange, and T. Mullin, J. Mech. Phys. Solids **56**, 2642 (2008).
[6] Y. Zhang, E. A. Matsumoto, A. Peter, P. C. Lin, R. D. Kamien, and S. Yang, Nano Lett. **8**, 1192 (2008).
[7] A. R. Parker and C. R. Lawrence, Nature **414**, 33 (2001).
[8] A. Thess, R. Lee, P. Nikolaev, H. J. Dai, P. Petit, J. Robert, C. H. Xu, Y. H. Lee, S. G. Kim, A. G. Rinzler, D. T. Colbert, G. E. Scuseria, D. Tomanek, J. E. Fischer, and R. E. Smalley, Science **273**, 483 (1996).
[9] M. J. Lopez, A. Rubio, J. A. Alonso, L. C. Qin, and S. Iijima, Phys. Rev. Lett. **86**, 3056 (2001).
[10] K. Zhang, T. Han, H. L. Duan, and J. Wang, Carbon **48**, 2948 (2010).
[11] R. H. Baughman, A. A. Zakhidov, and W. A. de Heer, Science **297**, 787 (2002).
[12] B. Gilbert, F. Huang, H. Z. Zhang, G. A. Waychunas, and J. F. Banfield, Science **305**, 651 (2004).
[13] G. Y. Jing, H. L. Duan, X. M. Sun, Z. S. Zhang, J. Xu, Y. D. Li, J. X. Wang, and D. P. Yu, Phys. Rev. B **73**, 235409 (2006).
[14] H. L. Duan, J. X. Wang, and B. L. Karihaloo, Adv. Appl. Mech. **42**, 1 (2008).
[15] B. Delley, J. Chem. Phys. **92**, 508 (1990).
[16] B. Delley, J. Chem. Phys. **113**, 7756 (2000).
[17] S. P. Chan, W. L. Yim, X. G. Gong, and Z. F. Liu, Phys. Rev. B **68**, 075404 (2003).
[18] S. P. Timoshenko and J. M. Gere, *Theory of Elastic Stability* (McGraw-Hill, New York, 1961).
[19] J. Z. Liu, Q. S. Zheng, L. F. Wang, and Q. Jiang, J. Mech. Phys. Solids **53**, 123 (2005).
[20] B. I. Yakobson, C. J. Brabec, and J. Bernholc, Phys. Rev. Lett. **76**, 2511 (1996).
[21] Y. Huang, J. Wu, and K. C. Hwang, Phys. Rev. B **74**, 245413 (2006).
[22] A. S. Vol′mir, *Stability of Deformable Systems* (Nauka, Moscow, 1967) (in Russian).
[23] J. Tersoff and R. S. Ruoff, Phys. Rev. Lett. **73**, 676 (1994).
[24] L. A. Girifalco, M. Hodak, and R. S. Lee, Phys. Rev. B **62**, 13104 (2000).
[25] J. E. Mark, *Polymer Data Handbook* (Oxford University Press, New York, 1999).
[26] S. P. Timoshenko and J. N. Goodier, *Theory of Elasticity* (McGraw-Hill, Tokyo, 1970).
[27] R. K. Oruganti and A. K. Ghosh, Acta Mater. **55**, 6074 (2007).

[28]J. Tang, L. C. Qin, T. Sasaki, M. Yudasaka, A. Matsushita, and S. Iijima, Phys. Rev. Lett. **85**, 1887 (2000).
[29]M. H. F. Sluiter, V. Kumar, and Y. Kawazoe, Phys. Rev. B **65**, 161402 (2002).
[30]X. W. Zhao, K. Zhang, J. X. Wang, and H. L. Duan, Math. Mech. Solids **15**, 744 (2010).
[31]D. Y. Sun, D. J. Shu, M. Ji, F. Liu, M. Wang, and X. G. Gong, Phys. Rev. B **70**, 165417 (2004).
[32]R. Hingmann and B. L. Marczinke, J. Rheol. **38**, 573 (1994).
[33]K. Zhang, H. L. Duan, B. L. Karihaloo, and J. X. Wang, Proc. Natl. Acad. Sci. U. S. A. **107**, 9502 (2010).
[34]J. A. Elliott, J. K. W. Sandler, A. H. Windle, R. J. Young, and M. S. P. Shaffer, Phys. Rev. Lett. **92**, 095501 (2004).
[35]J. C. Charlier, P. Lambin, and T. W. Ebbesen, Phys. Rev. B **54**, R8377 (1996).
[36]D. Chen, T. Sasaki, J. Tang, and L. C. Qin, Phys. Rev. B **77**, 125412 (2008).